QUARTERLY OF APPLIED MATHEMATICS

Vol. XXXI JANUARY, 1974 No. 4

THE TRANSIENT TEMPERATURE FIELD IN A COMPOSITE SEMI-SPACE RESULTING FROM AN INCIDENT HEAT FLUX*

By

P. B. GRIMADO

Bell Laboratories, Whippany, New Jersey 07981

Summary. The two-dimensional, transient temperature field in a composite semi-space resulting from an incident heat input is constructed using operational techniques. Examples of the temperature field are presented with general conclusions that allow a qualitative assessment of the temperature distribution given the heat input and thermal properties of the constituent materials.

1. Introduction. In the past decade considerable attention has been given to the study of the phenomenology of composite material behavior in many areas of engineering application. Undoubtedly this attention has been motivated by the ever-increasing sophistication of design concepts in which the engineer must seek to recast individual constituents, each not completely suited for the proposed application, and "create" in concert a composite configuration that possesses the desired engineering properties. In his quest for a viable composite configuration the engineer must rely on analyses to guide him, and consequently solutions to problems involving composite geometries in all aspects of engineering application are vital.

The subject of this paper concerns itself with the determination of the transient two-dimensional temperature field in the simplest of all composite configurations—a semi-space of two distinct materials. The solution to the problem presented herein is fundamental to the understanding of heat transfer in composite solids of a more complicated nature. Furthermore, the evaluation of thermal stresses is almost always preceded by a determination of the temperature field and hence the results that follow are directly applicable to this form of analysis.

Solutions to problems involving the conduction of heat in two distinct materials for heat flow described by a single spatial dimension have been extensively treated for both planar and cylindrical geometries, [1]. Thiruvenkatachar and Ramakushna [2] appear to be the first to consider the transient temperature field in two space dimensions in the case of a cylindrical composite. Kumar and Thiruvenkatachar [3], in their attempt

* Received October 18, 1972. This work has been performed under U. S. Army Contract DAHC60-71-C0005.

to improve the response of thermocouples and hot-wire anemometers, investigated the response of a finite composite cylinder to both radial and axial heat flow in the presence of harmonic variation of surface temperature. Kumar [4] considered the heat flow in a finite composite cylinder subjected to a temperature boundary condition used to simulate liquid-fuel rocket environments. Ölcer, in a series of papers [5–7], considers the problem of heat flow in a finite composite hollow circular cylinder. Solutions are obtained in a very general form for all conceivable boundary and initial conditions, although no solutions are explicitly constructed.

This paper is divided in the following manner: In Secs. 2 and 3 the problem is formulated and the solution obtained. The temperature at the contact surface point is recorded in terms of tabulated functions in Sec. 4, and in Sec. 5 some observations on the nature of the solution at this point are made. Some illustrative examples and qualitative assessment of the temperature field appear in Sec. 6; fiinally, conclusions are given in Sec. 7.

2. Formulation of the problem. Consider a half-space composed of two distinct materials (Fig. 1), one of which occupies the quarter-plane $x \geq 0$, $y > 0$ and the other the quarter-plane $x \geq 0$, $y < 0$. The surface of contact between the two materials is the plane $y = 0$ and the physical contact is assumed perfect. When the surface $x = 0$ is suddenly subjected to a heat input at a reference time $t = 0$ a transient two-dimensional temperature field will be established. It is assumed that this temperature field is governed by the Fourier heat conduction equations and therefore satisfies the following system of partial differential equations, boundary and initial conditions:

$$\kappa_1 \nabla^2 T_1 = \partial T_1/\partial t, \quad x > 0, \quad y < 0, \quad t > 0, \tag{1a}$$

$$\kappa_2 \nabla^2 T_2 = \partial T_2/\partial t, \quad x > 0, \quad y > 0, \quad t > 0, \tag{1b}$$

$$k_1\, \partial T_1(0, y, t)/\partial x = -Q_1(y, t), \quad y < 0, \quad t > 0, \tag{2a}$$

$$k_2\, \partial T_2(0, y, t)/\partial x = -Q_2(y, t), \quad y > 0, \quad t > 0, \qquad (2b)^1$$

$$\lim_{x\to\infty} T_1(x, y, t) = \lim_{x\to\infty} T_2(x, y, t) = 0, \qquad t \geq 0, \tag{3}$$

$$T_1(x, 0, t) = T_2(x, 0, t), \quad x \geq 0, \quad t \geq 0, \tag{4}$$

$$k_1\, \partial T_1(x, 0, t)/\partial y = k_2\, \partial T_2(x, 0, t)/\partial y, \qquad x \geq 0, \quad t \geq 0, \tag{5}$$

$$\lim_{y\to-\infty} T_1(x, y, t) \ \text{finite}, \qquad \lim_{y\to\infty} T_2(x, y, t) \ \text{finite}, \tag{6}$$

$$T_1(x, y, 0) = T_2(x, y, 0) = 0, \quad x \geq 0, \quad |y| \geq 0, \tag{7}$$

where $\nabla^2 \equiv \partial^2/\partial x^2 + \partial^2/\partial y^2$, $T(x, y, t)$ is the temperature, κ is the diffusivity, k is the conductivity and $Q(y, t)$ is the heat input. In addition, the quantities peculiar to region 1 ($x \geq 0$, $y < 0$) and region 2 ($x \geq 0$, $y > 0$) are distinguished by the appropriate subscript.

3. Method of solution. The solution to the problem formulated above is best pursued by the introduction of "dual transforms", i.e. the application of a Fourier-

[1] The introduction of a different functional dependence on the heat input is included for the sake of generality. Its physical significance can be envisioned when different surface absorption characteristics are admitted.

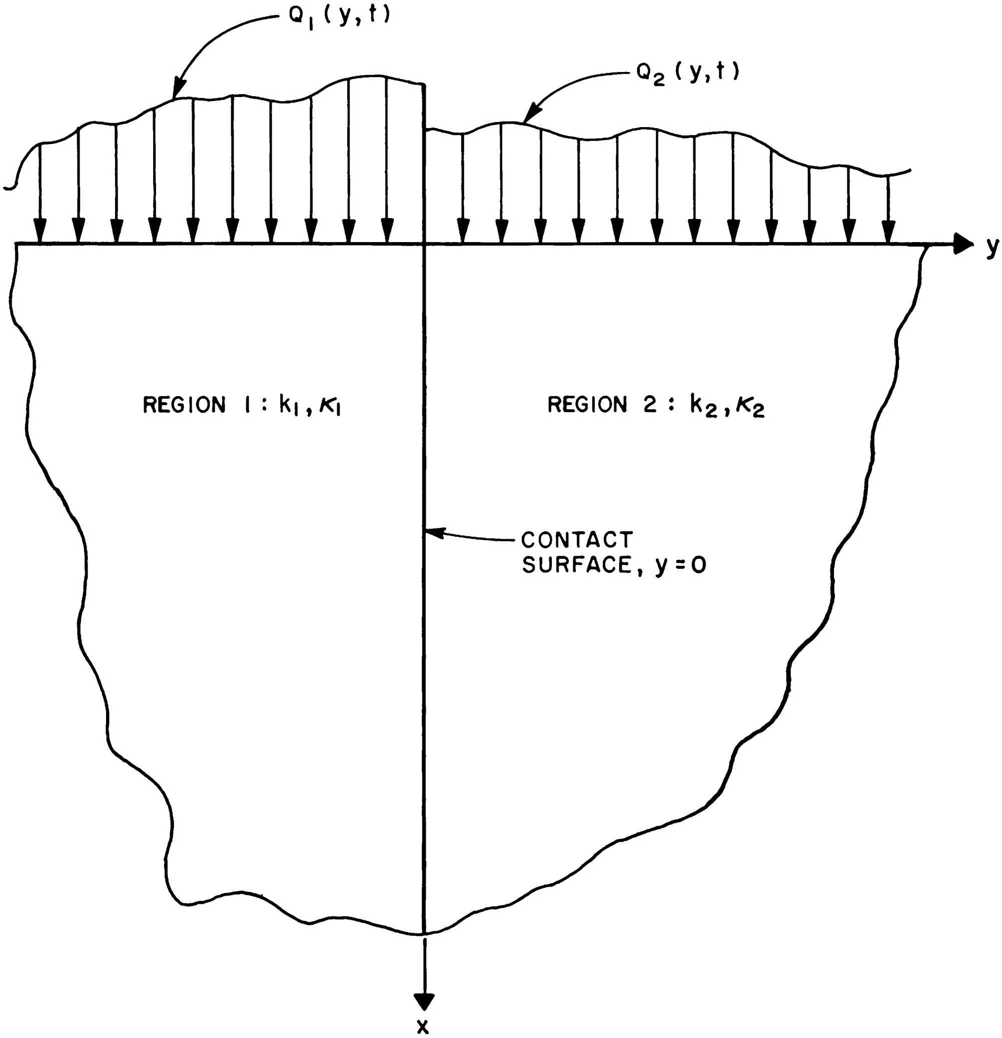

FIG. 1. Composite semi-space.

cosine transform on the spatial coordinate x followed by a Laplace transform made with respect to the time variable t.

The Fourier-cosine transform and Laplace transform of, say, $T(x, y, t)$ are defined as follows:

$$\bar{T}_C(y, t; \omega) = \int_0^\infty T(x, y, t) \cos \omega x \, dx; \qquad \bar{T}_L(x, y; p) = \int_0^\infty T(x, y, t) \exp(-pt) \, dt.$$

The dual transform of a function will be denoted by a double subscript: $\bar{T}_{CL}(y; \omega; p)$, indicating that a Fourier-cosine and a Laplace transform have been made. Conversely, the inversion of a dual transform function will be denoted by the symbol:

$$\{\bar{T}_{CL}(y; \omega; p)\}_{CL}^{-1} \equiv T(x, y, t).$$

Applying these integral transforms successively to Eqs. (1)–(7) results in the following system of equations:

$$\frac{d^2\bar{T}_{1CL}}{dy^2}(y;\omega;p) - (\omega^2 + p/\kappa_1)\bar{T}_{1CL}(y;\omega;p) = -Q_1/k_1p, \qquad y < 0, \tag{8}$$

$$\frac{d^2\bar{T}_{2CL}}{dy^2}(y;\omega;p) - (\omega^2 + p/\kappa_2)\bar{T}_{2CL}(y;\omega;p) = -Q_2/k_2p, \qquad y > 0, \tag{9}$$

$$\bar{T}_{2CL}(0;\omega;p) = \bar{T}_{1CL}(0;\omega;p), \tag{10}$$

and

$$k_1 \frac{\partial \bar{T}_{1CL}}{\partial y}(0;\omega;p) = k_2 \frac{\partial \bar{T}_{2CL}}{\partial y}(0;\omega;p), \tag{11}$$

where in Eqs. (8) and (9) the assumption has been made that the heat inputs Q_1 and Q_2 are constant[2] both spatially and temporally though in general unequal. The solution of the system of Eqs. (8)–(11) can be immediately given as:

$$\bar{T}_{1CL} = \frac{\exp[y(\omega^2 + p/\kappa_1)^{1/2}]}{k_1{}^2p(\omega^2 + p/\kappa_1)^{3/2}(\omega^2 + p/\kappa_2)^{1/2}} \left\{ \frac{Q_2k_1(\omega^2 + p/\kappa_1) - Q_1k_2(\omega^2 + p/\kappa_2)}{1 + (k_2/k_1)[(\omega^2 + p/\kappa_2)/(\omega^2 + p/\kappa_1)]^{1/2}} \right\} + Q_1/k_1p(\omega^2 + p/\kappa_1), \qquad y \le 0, \tag{12}$$

and in region 2

$$\bar{T}_{2CL} = \frac{-\exp[-y(\omega^2 + p/\kappa_2)^{1/2}]}{k_2k_1p(\omega^2 + p/\kappa_2)(\omega^2 + p/\kappa_1)} \left\{ \frac{Q_2k_1(\omega^2 + p/\kappa_1) - Q_1k_2(\omega^2 + p/\kappa_2)}{1 + (k_2/k_1)[(\omega^2 + p/\kappa_2)/(\omega^2 + p/\kappa_1)]^{1/2}} \right\} + Q_2/k_2p(\omega^2 + p/\kappa_2), \qquad y \ge 0. \tag{13}$$

The first expression on the right-hand side of (12) or (13) represents the two-dimensionality of the solution, whereas the second term is solely one-dimensional. The latter can be inverted once and for all without difficulty, using the inversion tables appearing in [8], to yield:

$$T_{j(x,t)}{}^{(1)} = \frac{2Q_j(\kappa_jt)^{1/2}}{k_j}\, i\mathrm{erfc}\,[x/2(\kappa_jt)^{1/2}], \qquad j = 1, 2, \tag{14}$$

where the subscript j is introduced to indicate the region of applicability, $i\mathrm{erfc}(x) \equiv \int_x^\infty \mathrm{erfc}(u)\,du$ with $\mathrm{erfc}(x) \equiv 2/\sqrt{\pi}\int_x^\infty \exp(-u^2)\,du$, commonly referred to as the complementary error function, while the superscript is employed to indicate the dimensionality of the solution.[3] This solution is nothing other than the temperature in the region $x \ge 0$ (semi-space) due to a constant heat input Q_j applied to the surface $x = 0$. To effect a dual inversion of the two-dimensional part of the temperature solution in the form given by (12) and (13) is extremely difficult. The form of these equations does, however, suggest some simplification providing we make the temporary restriction (ultimately to be relaxed):

---

[2] The case of arbitrary time-dependent heat inputs is accessible through the additional use of Duhamel's theorem [1].

[3] Clearly the complete solution, using this notation, could be written as $T_j(x, y, t) \equiv T_j{}^{(1)}(x, t) + T_j{}^{(2)}(x, y, t)$, $j = 1, 2$.

$$(k_2/k_1)^2 \, |(\omega^2 + p/\kappa_2)/(\omega^2 + p/\kappa_1)| < 1, \tag{15}$$

for then (12) and (13) can be recast in the form of a convergent series:

$$\bar{T}_{1CL}^{(2)} = \frac{\exp[y(\omega^2 + p/\kappa_1)^{1/2}][Q_2 k_1(\omega^2 + p/\kappa_1) - Q_1 k_2(\omega^2 + p/\kappa_2)]}{k_1^2 p(\omega^2 + p/\kappa_1)^{3/2}(\omega^2 + p/\kappa_2)^{1/2}} \cdot \sum_{n=0}^{\infty} [-(k_2/k_1)[(\omega^2 + p/\kappa_2)/(\omega^2 + p/\kappa_1)]^{1/2}]^n, \quad y \le 0, \tag{16}$$

and

$$\bar{T}_{2CL}^{(2)} = -\frac{\exp[-y(\omega^2 + p/\kappa_2)^{1/2}][Q_2 k_1(\omega^2 + p/\kappa_1) - Q_1 k_2(\omega^2 + p/\kappa_2)]}{k_2 k_1 p(\omega^2 + p/\kappa_2)(\omega^2 + p/\kappa_1)} \cdot \sum_{n=0}^{\infty} [-(k_2/k_1)[(\omega^2 + p/\kappa_2)/(\omega^2 + p/\kappa_1)]^{1/2}]^n, \quad y \ge 0. \tag{17}$$

Each and every term of the series (16) and (17) satisfies the differential Eqs. (8) and (9) and also the energy balance boundary condition (11), while the continuity of temperature, boundary condition (10), is satisfied when every term is accounted for.

Let us first concentrate for the moment on the inversion of $\bar{T}_{2CL}^{(2)}$. The generic expressions to be inverted in (17) are:

$$\frac{(\omega^2 + p/\kappa_2)^{n/2} \exp[-y(\omega^2 + p/\kappa_2)^{1/2}]}{p(\omega^2 + p/\kappa_1)^{n/2+1}}, \qquad \frac{(\omega^2 + p/\kappa_2)^{(n/2)-1} \exp[-y(\omega^2 + p/\kappa_2)^{1/2}]}{p(\omega^2 + p/\kappa_1)^{n/2}}, \qquad n = 0, 1, 2, \cdots. \tag{18}$$

The appearance of both κ_1 and κ_2 in these expressions precludes the direct use of inversion tables and hence resort must be had to a dual convolution integral to effect the inversion. The dual convolution integral, for example, applied to the transformed function $\{\bar{F}\bar{G}\}_{CL}$ can be written as:

$$\{\bar{F}\bar{G}\}_{CL}^{-1} = \frac{1}{2}\int_0^\infty \int_0^t g(\xi, \zeta)\{f(x + \xi, t - \zeta) + f(|x - \xi|, t - \zeta)\}\, d\zeta\, d\xi \tag{19}$$

where $f(x, t)$ and $g(x, t)$ are the dual inversions of $\bar{F}_{CL}$ and $\bar{G}_{CL}$ respectively. Having this procedure in mind, the first of (18) can be separated into two parts, one containing only the parameter κ_2 :

$$p^{-1}(\omega^2 + p/\kappa_2)^{n/2} \exp[-y(\omega^2 + p/\kappa_2)^{1/2}] \tag{20a}$$

and the other containing κ_1 :

$$(\omega^2 + p/\kappa_1)^{-n/2-1}. \tag{20b}$$

With the aid of the tables of [8], the inverse of (20a) and (20b) can be given as:

$$\{p^{-1}(\omega^2 + p/\kappa_2)^{n/2} \exp[-y(\omega^2 + p/\kappa_2)^{1/2}]\}_{CL}^{-1} = 2(\kappa_2 t)^{1/2}/\pi \int_1^\infty (\eta/4\kappa_2 t)^{(n/2)+1} H_{n+1}[y(\eta/4\kappa_2 t)^{1/2}] \exp[-\eta(x^2 + y^2)/4\kappa_2 t] \frac{d\eta}{\eta^{3/2}}$$

$$y > 0^{4}; \quad n = 0, 1, 2, \cdots, \tag{21a}$$

[4] This restriction is necessary since at $y = 0$ the expression on the left of (21a) has no definable inverse. We will see later on that this constraint disappears when the inverses of (20) are convolved.

and

$$\{(\omega^2 + p/\kappa_1)^{(-n/2)-1}\}_{CL}^{-1} = \kappa_1^{(n+1)/2}(t)^{(n-1)/2} \exp[-x^2/4\kappa_1 t]/\pi^{1/2}\Gamma((n/2)+1)$$

$$n = 0, 1, 2, \cdots, \qquad (21b)$$

where the function $H_n(x)$ is the Hermite polynomial and $\Gamma(x)$ is the gamma function.

Convolving Eqs. (21) in accordance with (19) permits us to write the inverse of the first of (18) as

$$\{p^{-1}(\omega^2 + p/\kappa_2)^{n/2}(\omega^2 + p/\kappa_1)^{(-n/2)-1} \exp[-y(\omega^2 + p/\kappa_2)^{1/2}]\}_{CL}^{-1}$$

$$= \frac{\kappa_1^{(n+1)/2}}{\pi^{3/2}\Gamma((n/2)+1)} \int_0^t \int_0^\infty (\kappa_2\zeta)^{1/2}(t-\zeta)^{(n-1)/2}$$

$$\cdot\left[\int_1^\infty (\eta/4\kappa_2\zeta)^{(n/2)+1}H_{n+1}[y(\eta/4\kappa_2\zeta)^{1/2}]\,\frac{\exp[-\eta(\xi^2+y^2)/4\kappa_2\zeta]}{\eta^{3/2}}\right] d\eta$$

$$\cdot[\exp[-(x+\xi)^2/4\kappa_1(t-\zeta)] + \exp[-(x-\xi)^2/4\kappa_1(t-\zeta)]]\, d\xi\, d\zeta,$$

$$y \geq 0, \quad n = 0, 1, 2, \cdots. \qquad (22)$$

Eq. (22) represents the inverse of the generic term (the term multiplied by the coefficient Q_1k_2) appearing in the infinite series of (17). The resulting series is capable of being expressed in closed form by first making the substitution

$$1/\Gamma((n/2)+1) = [2^{n+2}/\pi^{1/2}(n+1)!]\int_0^\infty u^{n+2}\exp(-u^2)\,du, \qquad n = 0, 1, 2, \cdots \qquad (23)$$

and then noticing that the sum is now of the form [9]:

$$\sum_{n=0}^{\infty}(-1)^n x^n H_n(y)/n! = \exp[2xy - x^2] \qquad (24)$$

which yields the desired closed-form expression. Performing the integrations with respect to the variables of integration u, ξ completes the inversion of the first of (18). The inversion of the second of (18) follows exactly the same procedure.

After first introducing the notation:

$$\mathfrak{D}(\kappa, X, Y) \equiv (2/\pi)$$

$$\cdot\int_1^K\int_0^\infty \exp[-nY^2(\xi^2+1) - X^2\eta(\xi^2+1)/(\eta\xi+1)]/[\eta(\xi^2+1)^{3/2}(\eta\xi^2+1)^{1/2}]\,d\xi\,d\eta, \qquad (25a)$$

$$\mathcal{E}(\kappa, k, X, Y) \equiv (2/\pi^{1/2})\int_1^\kappa\int_0^\infty \exp[-\eta Y^2(\xi^2+1) - X^2\eta(\xi^2+1)/(\eta\xi+1)]$$

$$\cdot\exp[(Yk\eta\xi)^2(\xi^2+1)/(k^2\eta\xi^2+1)]\,i\mathrm{erfc}$$

$$\cdot\{Y\eta[k^2\xi^2(\xi^2+1)/(k^2\eta\xi^2+1)]^{1/2}\}/[\eta(\xi^2+1)^{3/2}(k^2\eta\xi^2+1)(\eta\xi^2+1)^{1/2}]\,d\xi\,d\eta \qquad (25b)$$

and the identities[5]

[5] Eqs. (26) follow from the equivalence of a "direct" inversion of a dual transformed function and the same function inverted using the dual convolution integral.

$$\mathfrak{D}(\infty, X, Y) = \int_1^\infty \exp(-nX^2) \operatorname{erfc}(Y\sqrt{\eta})\eta^{-3/2}\, d\eta, \tag{26a}$$

$$\mathcal{E}(\infty, k, X, Y) = (1 + k)^{-1}\mathfrak{D}(\infty, X, Y), \tag{26b}$$

we are then finally able to present the temperature in region 2 as:

$$\begin{aligned} &k_2\pi^{1/2}T_2(X, Y, t)/4Q_2(\kappa_2 t)^{1/2} \\ &\quad = -\mathfrak{D}(\infty, X, Y)/4 + [\kappa_{12}^{1/2}(Q_{12} + 1)/4(k_{12} + 1)]\mathfrak{D}(\infty, X\kappa_{21}^{1/2}, Y\kappa_{21}^{1/2}) \\ &\quad\quad - [\kappa_{12}^{1/2}(k_{21} - Q_{12})/4]\,\mathcal{E}(\kappa_{12}, k_{21}, X, Y) \\ &\quad\quad + [\kappa_{12}^{1/2}Q_{12}/4]\mathfrak{D}(\kappa_{12}, X\kappa_{21}^{1/2}, Y\kappa_{21}^{1/2}) + \pi^{1/2} i\operatorname{erfc}(X)/2, \qquad X \geq 0, \quad Y \geq 0 \end{aligned} \tag{27}$$

where in (27) the following nondimensional quantities have been introduced:

$$X^2 \equiv x^2/4\kappa_2 t; \qquad Y^2 \equiv y^2/4\kappa_2 t; \qquad Q_{12} \equiv Q_1/Q_2;$$

$$k_{12} \equiv k_1/k_2; \qquad \kappa_{12} \equiv \kappa_1/\kappa_2; \qquad \kappa_{21} \equiv \kappa_2/\kappa_1; \qquad k_{21} \equiv k_2/k_1.$$

The temperature in region 1 is derived from that of region 2 by simply noting that the solution is invariant to material interchange, i.e. region 1 $\leftrightarrow$ region 2. The solution applicable to region 1 then follows immediately from (27) after permuting the indices and is given as:

$$\begin{aligned} &k_2\pi^{1/2}T_1(X, Y, t)/4Q_2(\kappa_2 t)^{1/2} \\ &\quad = -(Q_{12}k_{21}\kappa_{12}^{1/2}/4)\mathfrak{D}(\infty, X\kappa_{21}^{1/2}, |Y|\,\kappa_{21}^{1/2}) + [(Q_{12} + 1)/4(k_{12} + 1)]\mathfrak{D}(\infty, X, |Y|) \\ &\quad\quad - [(Q_{12} - k_{21})/4]\,\mathcal{E}(\kappa_{21}, k_{12}, X, |Y|) - (k_{21}/4)\mathfrak{D}(\kappa_{21}, X, |Y|) \\ &\quad\quad + Q_{12}k_{21}(\pi\kappa_{12})^{1/2} i\operatorname{erfc}(X\kappa_{21}^{1/2})/2, \qquad X \geq 0, \quad Y \leq 0. \end{aligned} \tag{28}$$

It is to be noted here that the methodology employed does not require the satisfaction of inequality (15) as a necessary ingredient. For if this were violated the denominator of Eqs. (12) and (13) could have been put into the form:

$$1 + (k_1/k_2)[(\omega^2 + p/\kappa_1)/(\omega^2 + p/\kappa_2)]^{1/2}.$$

Expanding in a manner similar to that used and performing the inversions as outlined above would yield the same solution as that given by Eqs. (27) and (28).

4. Temperature at the surface contact point $X = Y = 0$. At the point $X = Y = 0$ the integrals appearing in Eqs. (27) and (28) can be evaluated in terms of tabulated functions. The temperature at this point is interesting in itself and is therefore recorded below. Note that in what follows:

$$\tilde{T}_0 \equiv k_2\pi^{1/2}T(0, 0, t)/4Q_2(\kappa_2 t)^{1/2};$$

$$\tilde{\kappa}_{12} = (1 - \kappa_{12})^{1/2}; \qquad \tilde{\kappa}_{21} = (1 - \kappa_{21})^{1/2};$$

$$\rho_1 = [(1 - k_{12}^2)(1 - \kappa_{21}k_{12}^2)]^{-1/2}; \qquad \rho_2 = [(1 - k_{12}^2)(\kappa_{21}k_{12}^2 - 1)]^{-1/2};$$

$$\rho_3 = [(k_{12}^2 - 1)(\kappa_{21}k_{12}^2 - 1)]^{-1/2}; \qquad \rho_4 = [(k_{12}^2 - 1)(1 - \kappa_{21}k_{12}^2)]^{-1/2};$$

$$\beta_1 = \sin^{-1}(k_{12}\kappa_{21}^{1/2}); \qquad \beta_2 = \sin^{-1}[(1 - k_{12}^2)/(1 - \kappa_{12})]^{1/2};$$

$$\beta_3 = \sin^{-1}[\kappa_{21}(1 - k_{12}^2)/(1 - k_{12}^2\kappa_{21})]^{1/2}; \quad \beta_4 = \sin^{-1}[(1 - \kappa_{21}k_{12}^2)/(1 - \kappa_{21})]^{1/2};$$

$$\beta_5 = \sin^{-1}[(k_{12}^2\kappa_{21} - 1)/\kappa_{21}(k_{12}^2 - 1)]^{1/2}; \qquad \beta_6 = \sin^{-1} k_{12};$$

$\Lambda_0(\beta, k)$ is Heuman's lambda function and is tabulated in [10] and [11]; $Z(\beta, k)$ is the Jacobian zeta function and is tabulated in [10] and [12]; $K(k)$ and $E(k)$ are the complete elliptic integrals of the first and second kind, respectively and these are tabulated in [9–12].

$$\kappa_{21} > 1, \quad k_{21} > 1$$

(1) $\kappa_{21} < k_{21}^2$:

$$\tilde{T}_0 = (Q_{12}\kappa_{12}^{1/2}/\pi)K(\tilde{\kappa}_{12}) + [\rho_1(1 - Q_{12}k_{12})/2][1 - \Lambda_0(\beta_1, \tilde{\kappa}_{12})]. \tag{29}$$

(2) $\kappa_{21} > k_{21}^2$:

$$\tilde{T}_0 = (Q_{12}\kappa_{12}^{1/2}/\pi)K(\tilde{\kappa}_{12}) + [\rho_2(1 - Q_{12}k_{12})/\pi]Z(\beta_2, \tilde{\kappa}_{12}). \tag{30}$$

(3) $\kappa_{21} = k_{21}^2$:

$$\tilde{T}_0 = (Q_{12}\kappa_{12}^{1/2}/\pi)K(\tilde{\kappa}_{12}) + [(1 - Q_{12}\kappa_{12}^{1/2})/\pi\tilde{\kappa}_{12}^2][E(\tilde{\kappa}_{12}) - \kappa_{12}K(\tilde{\kappa}_{12})]. \tag{31}$$

$$\kappa_{21} > 1, \quad k_{21} \leq 1$$

(1) $k_{21} = 1$:

$$\tilde{T}_0 = (Q_{12}\kappa_{12}^{1/2}/\pi)K(\tilde{\kappa}_{12}) + [(1 - Q_{12})\kappa_{12}^{1/2}/\pi\tilde{\kappa}_{12}^2][K(\tilde{\kappa}_{12}) - E(\tilde{\kappa}_{12})]. \tag{32}$$

(2) $k_{21} < 1$:

$$\tilde{T}_0 = (Q_{12}\kappa_{12}^{1/2}/\pi)K(\tilde{\kappa}_{12}) + [(1 - Q_{12}k_{12})\kappa_{12}^{1/2}/\pi k_{12}][K(\tilde{\kappa}_{12})/(1 - k_{21}^2\kappa_{12}) - \pi\rho_3\Lambda_0(\beta_3, \tilde{\kappa}_{12})/2k_{12}\kappa_{21}^{1/2}]. \tag{33}$$

$$\kappa_{21} < 1, \quad k_{21} < 1$$

(1) $\kappa_{21} < k_{21}^2$:

$$\tilde{T}_0 = (Q_{12}/\pi)K(\tilde{\kappa}_{21}) + [\rho_4(1 - k_{12}Q_{12})/\pi]K(\tilde{\kappa}_{21})Z(\beta_4, \tilde{\kappa}_{21}). \tag{34}$$

(2) $\kappa_{21} > k_{21}^2$:

$$\tilde{T}_0 = (Q_{12}/\pi)K(\tilde{\kappa}_{21}) + [(1 - Q_{12}k_{12})/\pi k_{21}][K(\tilde{\kappa}_{21})/(k_{12}^2 - 1) - \pi\rho_3\Lambda_0(\beta_5, \tilde{\kappa}_{21})/2k_{12}]. \tag{35}$$

(3) $\kappa_{21} = k_{21}^2$:

$$\tilde{T}_0 = (Q_{12}/\pi)K(\tilde{\kappa}_{21}) + [(1 - Q_{12}k_{12})/\pi k_{12}\tilde{\kappa}_{21}^2][K(\tilde{\kappa}_{21}) - E(\tilde{\kappa}_{21})]. \tag{36}$$

$$\kappa_{21} < 1, \quad k_{21} \geq 1$$

(1) $k_{21} = 1$:

$$\tilde{T}_0 = (Q_{12}/\pi)K(\tilde{\kappa}_{21}) - [(1 - Q_{12})/\pi\tilde{\kappa}_{21}^2][\kappa_{21}K(\tilde{\kappa}_{21}) - E(\tilde{\kappa}_{21})]. \tag{37}$$

(2) $k_{21} > 1$:

$$\tilde{T}_0 = (Q_{12}/\pi)K(\tilde{\kappa}_{21}) + [\rho_1(1 - Q_{12}k_{12})][1 - \Lambda_0(\beta_6, \tilde{\kappa}_{21})]. \tag{38}$$

$$\kappa_{21} = 1, \ k_{21} \text{ arbitrary}$$

$$\tilde{T}_0 = (1 + Q_{12})/2(1 + k_{12}). \tag{39}$$

5. Observations on the nature of the solution at the surface contact point $X = Y = 0$. Numerical evaluation of the temperature at the contact point, $X = Y = 0$, exploiting Eqs. (29–39) for particular choices of the parameters Q_{12}, k_{12}, and κ_{12}, implies that this temperature is bounded by the temperature at $X = 0$ and $|Y| \to \infty$, the one-dimensional half-space solution. Although this property of the solution can be rigorously proven only for the choice of parameters given by (39), it does not appear to be unreasonable when extended to include all possible parametric variations; besides, ad hoc verification is always available through Eqs. (29–39). In terms of the parameters of the formulation this condition can be mathematically stated as:

$$[\tfrac{1}{2}, Q_{12}k_{21}\kappa_{12}{}^{1/2}/2]_{\min} < k_2\pi^{1/2}T(0, 0, t)/4Q_2(\kappa_2 t)^{1/2} < [\tfrac{1}{2}, Q_{12}k_{21}\kappa_{12}{}^{1/2}/2]_{\max} \qquad (40a)$$

and for the special case $Q_{12}k_{21}\kappa_{12}{}^{1/2} = 1$ the above would be replaced by the inequality:

$$k_2\pi^{1/2}T(0, 0, t)/4Q_2(\kappa_2 t)^{1/2} \leq \tfrac{1}{2}. \qquad (40b)$$

Let us now examine the transfer of heat at this point. To this end, we can express the heat flow from either Eqs. (27) or (28) in the y-direction as:

$$(\pi k_2/Q_2)\frac{\partial T_2}{\partial y}(0, 0, t)$$

$$= \lim_{Y\to 0}\frac{1}{(k_{21}+1)}\{(Q_{12}k_{21} - 1)[\ln (Y^2) + \gamma] - k_{21}(Q_{12} + 1)\ln (\kappa_{21})\}$$

$$- \pi^{1/2}[\kappa_{12}{}^{1/2}(k_{21} - Q_{12})/2]\frac{\partial \mathcal{E}}{\partial Y}(\kappa_{12}, k_{21}, 0, 0) + 0(Y^2) \qquad (41)$$

where $\gamma = .577215 \cdots$ is Euler's constant. The transfer of heat between regions 1 and 2 at the point $X = Y = 0$ is seen to be logarithmically singular except for the special case of proportional heating, $Q_{12}k_{21} = 1$. The direction of this singular heat transfer rate is determined only by the parametric combination $Q_{21}k_{21}$ and immediately three situations can be distinguished:

1. $$Q_{12}k_{21} > 1: \quad k_2\partial T_2(0, 0, t)/\partial y = -\infty, \qquad (42a)$$
2. $$Q_{12}k_{21} < 1: \quad k_2\partial T_2(0, 0, t)/\partial y = \infty, \qquad (42b)$$
3. $$Q_{12}k_{21} = 1: \quad (\pi k_2/Q_2)\frac{\partial T_2}{y\partial}(0, 0, t) = [(Q_{12} + 1)/(k_{12} + 1)]\ln (\kappa_{21})$$
$$- \pi^{1/2}[\kappa_{12}{}^{1/2}(k_{12} - Q_{12})/2]\frac{\partial \mathcal{E}}{\partial Y}(\kappa_{12}, k_{21}, 0, 0). \qquad (42c)$$

6. Qualitative assessment of the temperature field with some examples. Let us now examine the temperature distribution and how it is influenced by the parameters of the problem. Several cases can be delineated toward this end:

(1) $Q_{12}k_{21} > 1$, $Q_{12}k_{21}\kappa_{12}{}^{1/2} > 1$. The first condition, from (42a), implies $\partial T_i(0, 0, t)/\partial y = -\infty$, while the second states that on $X = 0$ the far-field temperature ($|Y| \to \infty$) in region 1 is larger than that in region 2. As stated in (40), the temperature at $X = Y = 0$ is bounded by the far-field temperature and hence it would appear that a smooth transition from this point to the far-field can be accomplished with a monotonic increasing gradient. Consequently, nowhere on the surface $X = 0$ can the temperature fall outside the bounds provided by the far-field. Fig. 2 presents the temperature for

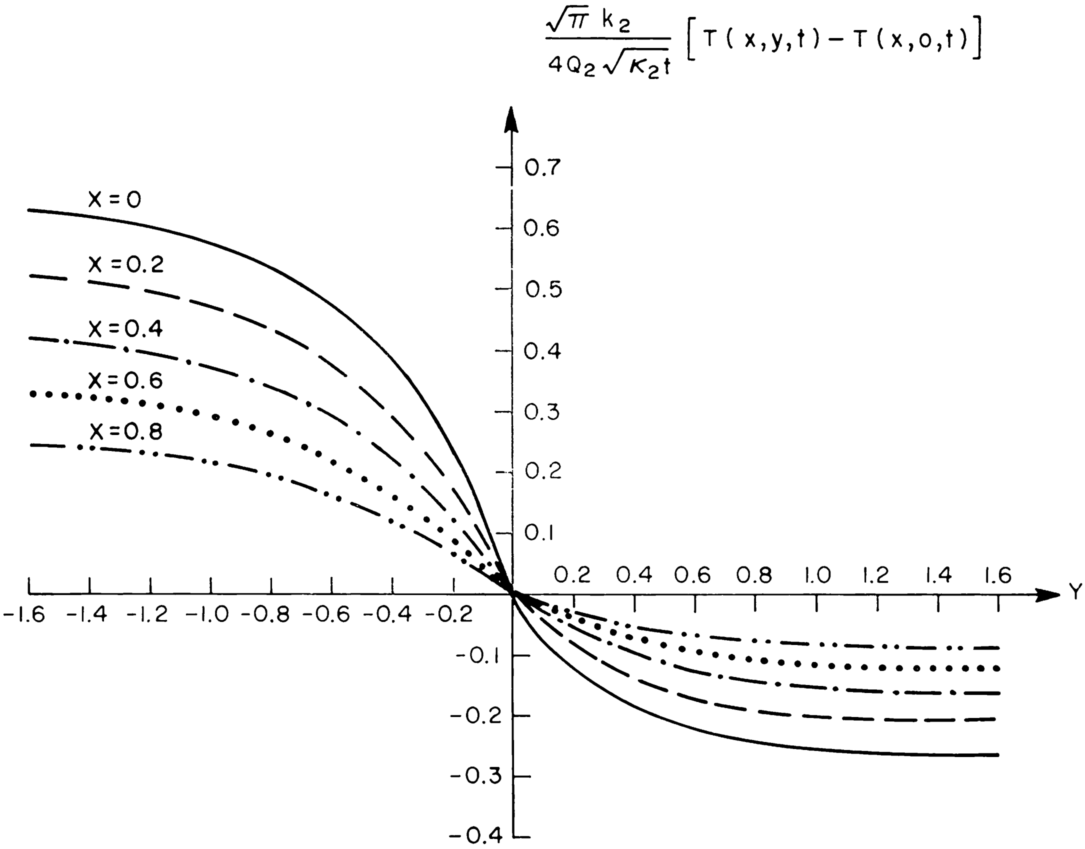

FIG. 2. Temperature profiles for $Q_{12} \doteq 1$, $k_{21} = 2$ and $k_{21}{}^2\kappa_{12} = 8$.

parameters $Q_{12} = 1$, $k_{21} = 2$ and $\kappa_{12} = 2$. It is immediately apparent that all the properties of the solution cited above are substantiated. These properties, however, may or may not be fulfilled when $X > 0$. It will be seen in what follows that the temperature profile for $X > 0$ is influenced by the diffusivity ratio κ_{12}.

The second inequality that distinguishes this case permits κ_{12} to be either greater than or less than unity; let us assume the latter condition, i.e. $\kappa_{12} < 1$. Now, writing the difference in the far-field temperature in region 1 and region 2, we have

$$[k_2\pi^{1/2}/4Q_2(\kappa_2 t)^{1/2}][T_1(X, -\infty, t) - T_2(X, \infty, t)]$$
$$= \tfrac{1}{2}[Q_{12}k_{21}\kappa_{12}{}^{1/2} i\mathrm{erfc}\ (X\kappa_{21}{}^{1/2}) - i\mathrm{erfc}\ (X)]. \qquad (43)$$

It can be shown that there exists an $X^* > 0$ such that, for $0 \leq X < X^*$, Eq. (43) gives $T_1(x, -\infty, t) > T_2(x, \infty, t)$; however, when X becomes sufficiently large, the functions i erfc $(X\kappa_{21}{}^{1/2})$ and i erfc (X) dominate with the former becoming smaller to the extent that for $X \geq X^*$, we find $T_1(x, -\infty, t) \leq T_2(x, \infty, t)$. We would therefore expect, based on the previous discussion for $X = 0$, that the temperature profile in the neighborhood of $X = X^*$ will differ markedly from that already observed for $X = 0$. Drawing attention to Table 1, where $T(x, 0, t)$, $k_i\ \partial T_i(x, 0, t)/\partial y$, and $T_i(x, \pm\infty, t)$ are given for $Q_{12} = 1$, $k_{21} = 6$, and $\kappa_{12} = 1/2$, we see that the far-field temperature in regions 1 and 2 are equal at approximately $X = 1$. Also notice that the temperature on the interface $Y = 0$ is bounded by the far-field *except* in the range $1 \leq X \leq 1.3$ where the temperature is seen to exceed the far-field, whereas the gradient passes through zero and and subsequently undergoes a sign change at approximately $X = .75$. We would then anticipate that within the range $.75 \leq X \leq 1.3$ there will be a "transition zone" in which the temperature distribution goes from one generic shape to another. Fig. 3 confirms this hypothesis. There the temperature distribution is displayed for several values of X and we note that a transition zone appears located with the range $.75 < X < 1.3$ and within it the shape of the temperature profile assumes what we shall call, for lack of a better descriptive word, a "wiggle". This can be generically characterized by the attainment of a zero gradient at some finite value of Y. Outside this zone it appears that the temperature in region 1 approaches its far-field value in a monotonic fashion. On the other hand, in region 2 a slight wiggle persists to a value $X = 2.5$, the point at which calculations ceased.

TABLE 1

Temperature and gradient at the contact surface $Y = 0$ and far-field temperature for $Q_{12} = 1$, $k_{21} = 6$ and $\kappa_{21} = 2$.

$\frac{X}{2\sqrt{\kappa_2 t}}$	$\frac{\sqrt{\pi}\, k_2 T(X,0,t)}{4Q_2\sqrt{\kappa_2 t}}$	$\frac{\pi k_2}{Q_2} \frac{\partial T_2(X,0,t)}{\partial y}$	$\frac{\sqrt{\pi}\, k_2 T_1(X,-\infty,t)}{4Q_2\sqrt{\kappa_2 t}}$	$\frac{\sqrt{\pi}\, k_2 T_2(X,\infty,t)}{4Q_2\sqrt{\kappa_2 t}}$
0.0	0.765	$-\infty$	2.121	0.500
0.10	0.624	−2.115	1.631	0.416
0.20	0.496	−1.178	1.225	0.342
0.30	0.393	−0.684	0.896	0.278
0.40	0.306	−0.385	0.639	0.223
0.50	0.235	−0.198	0.443	0.176
0.60	0.177	-0.816×10^{-1}	0.298	0.138
0.70	0.132	-0.145×10^{-1}	0.194	0.106
0.80	0.969×10^{-1}	0.211×10^{-1}	0.123	0.808×10^{-1}
0.90	0.699×10^{-1}	0.369×10^{-1}	0.759×10^{-1}	0.604×10^{-1}
1.00	0.497×10^{-1}	0.407×10^{-1}	0.451×10^{-1}	0.445×10^{-1}
1.10	0.348×10^{-1}	0.379×10^{-1}	0.259×10^{-1}	0.323×10^{-1}
1.20	0.240×10^{-1}	0.322×10^{-1}	0.144×10^{-1}	0.230×10^{-1}
1.30	0.163×10^{-1}	0.257×10^{-1}	0.778×10^{-2}	0.162×10^{-1}
1.40	0.109×10^{-1}	0.195×10^{-1}	0.404×10^{-2}	0.112×10^{-1}
1.50	0.722×10^{-2}	0.143×10^{-1}	0.203×10^{-2}	0.764×10^{-2}

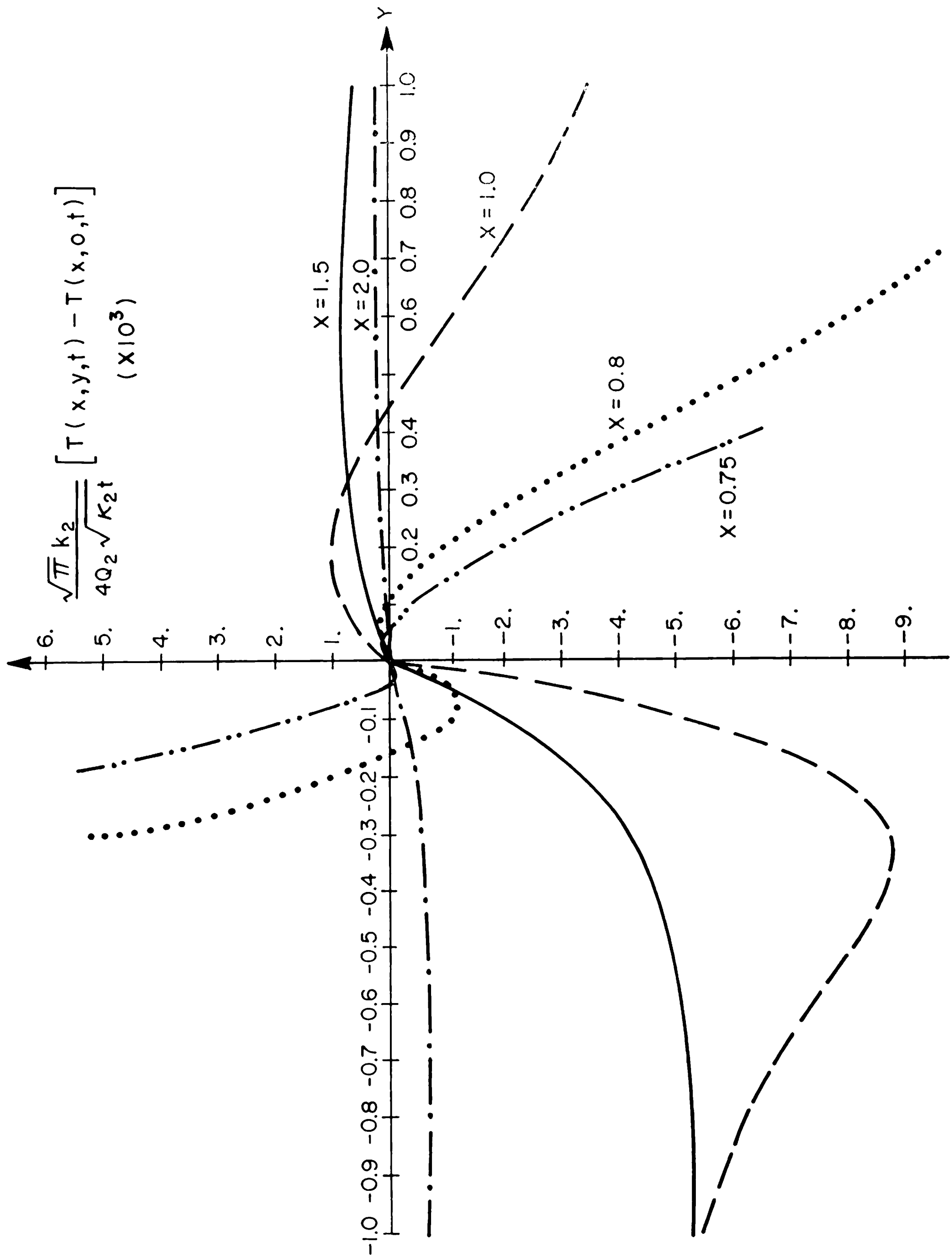

FIG. 3. Temperature profile for $Q_{12} = 1$, $k_{21} = 6$ and $k_{21}{}^2\kappa_{12} = 18$.

When $\kappa_{12} > 1$ Eq. (43) is always greater than zero and hence $T_1(x, -\infty, t) > T_2(x, \infty, t)$ for all values of X. It is therefore to be expected that the temperature profile for $X \geq 0$ will be of a similar nature. To illustrate this, Figure 2 gives the temperature distribution for various values of X for $Q_{12} = 1$, $k_{21} = 2$, and $\kappa_{12} = 2$.

(2) $Q_{12}k_{21} < 1$; $Q_{12}k_{21}\kappa_{12}^{1/2} \leq 1$. This condition can be simply arrived at by taking the reciprocal of the Case (1) parameters, yielding the mirror-image of the temperature obtained in case (1). Clearly, with only obvious modifications, all observations made for case (1) are equally valid here.

(3) $Q_{12}k_{21} < 1$; $Q_{12}k_{21}\kappa_{12}^{1/2} \geq 1$. From (42b) the first inequality implies that $\partial T_i/\partial_y(0, 0, t) = +\infty$, while the second condition states that the far-field temperature on the surface $X = 0$ in region 1 is equal to or greater than that in region 2. Eqs. (40) with the above properties imply that a smooth transition from the contact point $X = Y = 0$ to the far-field can be effected only if the temperature, as in the previous case, has a wiggle profile. Unlike case (1) and case (2), however, this combination of parameters permits no *a priori* bounds on the surface temperature for $|Y| > 0$. To illustrate this case we chose the following combination of parameters: $Q_{12} = 1$, $k_{21} = 1/2$ and $k_{21}\kappa_{12}^{1/2} = 10^{1/2}/2$. The results of the numerical calculations are plotted in Fig. 4. On $X = 0$ the maximum temperature in region 2 exceeds the far-field temperature by about 20% and is realized, as seen in Fig. 4, at $Y \simeq .005$. The wiggle temperature profile persists to about $X = .04$[6], beyond which it degenerates to one similar to case (1) (with $\kappa_{12} > 1$).

(4) $Q_{12}k_{21} > 1$; $Q_{12}k_{21}\kappa_{12}^{1/2} \leq 1$. This selection of parameters creates on $X = 0$ a temperature that is also characterized by a wiggle, the mirror-image of that given by case (3) since the parameters are the reciprocal of the case (3) parameters. With only obvious modifications the general comments made for case (3) are also valid here.

7. Conclusions. A solution for the temperature field in a composite semi-space has been obtained. This solution is expressed in terms of integrals which can be evaluated as shown by the illustrative cases presented. In particular, at the contact surface point $X = Y = 0$ the temperature is explicitly given in terms of tabulated functions.

From the illustrative problems presented, it appears that the following generalization can be made: the temperature distribution on the surface $X = 0$ can be characterized in a qualitative sense by the parametric combinations $Q_{12}k_{21}$ and $Q_{12}k_{21}\kappa_{12}^{1/2}$. Furthermore, the temperature does not, in general, retain the same shape for all $X > 0$ but instead goes through a finite transition zone in which the temperature experiences what we have previously described as a wiggle profile. Beyond this zone the temperature field assumes a shape that remains unaltered. Although, as cited above, only two parametric combinations affect the temperature profile on $X = 0$, a third quantity, namely the diffusivity ratio κ_{12}, strongly influences the profile for $X > 0$. In fact it is to be expected that the combinations:

$$Q_{12}k_{21} < 1; \quad Q_{12}k_{21}\kappa_{12}^{1/2} < 1; \quad \kappa_{12} < 1$$

or (44)

$$Q_{12}k_{21} > 1; \quad Q_{12}k_{21}\kappa_{12}^{1/2} > 1; \quad \kappa_{12} > 1$$

will be the only families of parameters which result in a temperature profile devoid of a wiggle or transition zone. Whenever one of the inequalities defined in (44) is violated, a transitional zone can be anticipated. In particular, when either $Q_{12}k_{21} < 1$ and $Q_{12}k_{21}\kappa_{12}^{1/2} > 1$, or $Q_{12}k_{21} > 1$ and $Q_{12}k_{21}\kappa_{12}^{1/2} < 1$, a wiggle temperature distribution

[6] This value at which the temperature profile undergoes a change in shape can be ascertained as the value of X at which the gradient goes through zero.

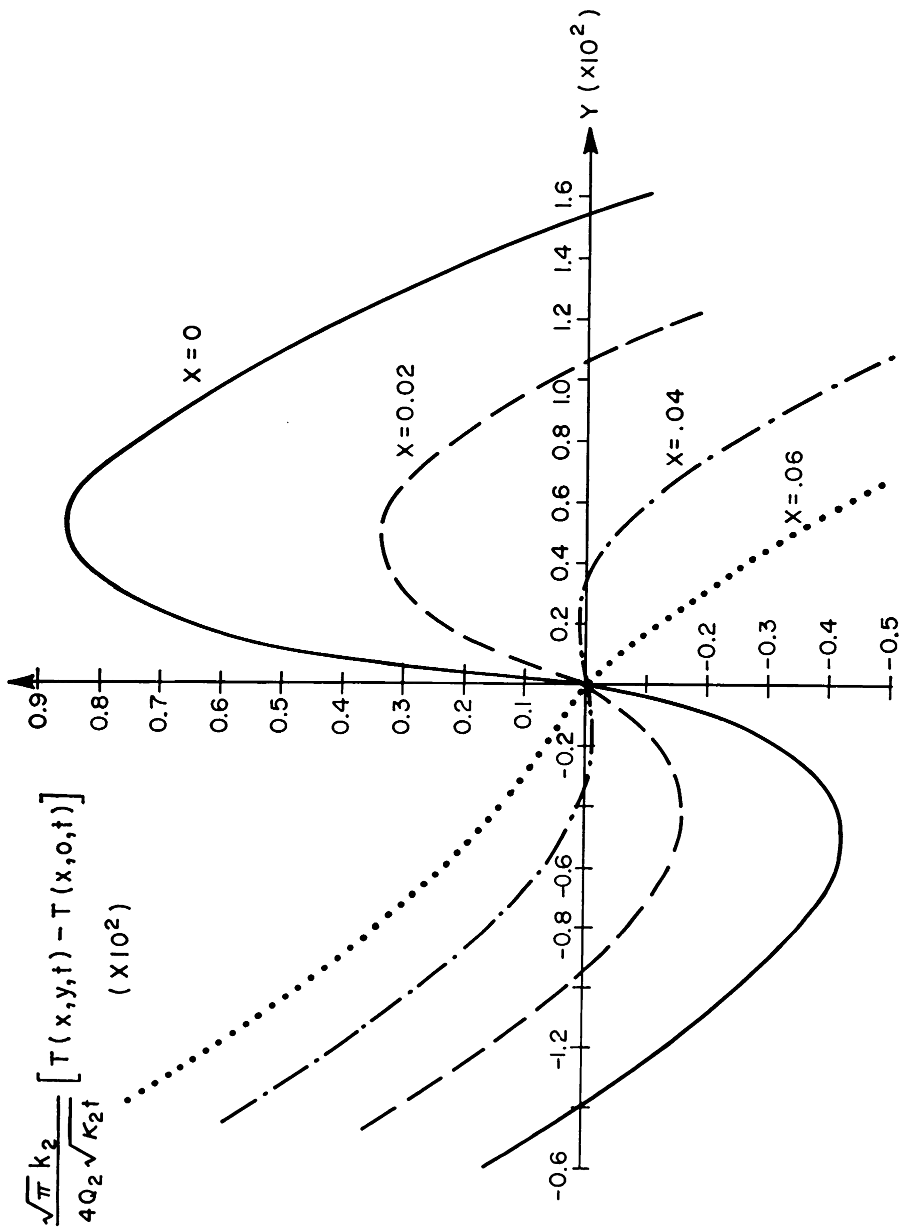

Fig. 4. Temperature profiles for $Q_{12} = 1$, $k_{21} = \frac{1}{2}$ and $k_{21}^2\kappa_{12} = \frac{10}{4}$.

is initiated on the top surface $X = 0$ and extends into the body, the actual distance being dependent on the numerical values of the parameters. On the other hand, for the case $Q_{12}k_{21} < 1$, $Q_{12}k_{21}\kappa_{12}^{1/2} < 1$ and $\kappa_{12} > 1$, or $Q_{12}k_{21} > 1$, $Q_{12}k_{21}\kappa_{12}^{1/2} > 1$ and $\kappa_{12} < 1$, the surface $X = 0$ will not experience a wiggle profile. Nevertheless, a transition zone will be established within the body, the location being *a priori* estimated[7] to be

[7] This estimate is based on the results of the example presented. The precise location at which this profile can be expected to originate is given by the value of X that satisfies $\partial T(x, 0, t)/\partial y = 0$.

in the vicinity of the value of X that equalizes the far-field temperature in regions 1 and 2.

In conclusion, it is worthy of note that the solutions presented herein for the composite semi-space can be extended to include the geometry of a composite slab, i.e. one with finite thickness with the back surface thermally insulated, by making use of the well-known method of images [1].

References

[1] H. S. Carslaw and J. C. Jaeger, *Conduction of heat in solids*, Clarendon Press, Oxford, England, 1959

[2] V. R. Thiruvenkatachar and B. S. Ramakushna, *A case of combined radial and axial heat flow in composite cylinders*, Quart. Appl. Math. **10**, 255–262 (1952)

[3] I. J. Kumar and V. R. Thiruvenkatachar, *Heat flow in a finite composite cylinder by harmonic variation of surface temperature*, Indian J. Math. **3**, 47–62 (1961)

[4] I. J. Kumar, *Heat flow in hollow composite cylinders*, Proc. Nat. Inst. Sci. India **29**, 452–459 (1963)

[5] N. Y. Ölcer, *On a heat flow problem in a hollow circular cylinder*, Proc. Camb. Phil. Soc. **64**, 193–202 (1968)

[6] N. Y. Ölcer, *A general class of unsteady heat flow problems in a finite composite hollow circular cylinder*, Quart. Appl. Math. **26**, 355–371, (1968)

[7] N. Y. Ölcer, *A general unsteady heat flow problem in a finite composite hollow circular cylinder under boundary conditions of the second kind*, Nuclear Engr. Des. **7**, 97–112 (1968)

[8] A. Erdélyi et al., *Tables of integral transforms*, Vol. 1, McGraw–Hill, New York, 1954

[9] M. Abramowitz and I. A. Stegun, *Handbook of mathematical functions with formulas, graphs and mathematical tables*, National Bureau of Standards, Applied Mathematics Series, 55, 1965

[10] P. F. Byrd and M. D. Friedman, *Handbook of elliptic integrals for engineers and scientists*, second edition, revised, Springer–Verlag, New York, 1971

[11] C. Heuman, *Tables of complete elliptic integrals*, J. Math Phys. **20**, 127–206 (1941)

[12] L. M. Milne-Thomson, *Jacobian elliptic function tables*, Dover, New York, 1950